

1 ***INTERMEDIUM-C* mediates the shade-induced bud growth arrest in barley**

2

3 Hongwen Wang^{1,2,*}, Christiane Seiler², Nese Sreenivasulu³, Nicolaus von Wirén^{1,*} and Markus
4 Kuhlmann^{2,*}

5

6 ¹Department of Physiology and Cell Biology, Leibniz Institute of Plant Genetics and Crop Plant
7 Research (IPK) Gatersleben, Corrensstrasse 3, 06466 Stadt Seeland, Germany

8 ²Department of Molecular Genetics, Leibniz Institute of Plant Genetics and Crop Plant Research (IPK)
9 Gatersleben, Corrensstrasse 3, 06466 Stadt Seeland, Germany

10 ³International Rice Research Institute (IRRI), Grain Quality and Nutrition Center, Metro Manila,
11 Philippines

12

13 **Running title:** Genetic control of shade-induced bud growth arrest

14

15 **Correspondence to:** Hongwen Wang (email: wangh@ipk-gatersleben.de), Nicolaus von
16 Wirén (email: vonwiren@ipk-gatersleben.de) and Markus Kuhlmann (email: Kuhlmann@ipk-gatersleben.de)

17

18 **Tel:** +49-0394825-172 or +49-0394825-602

19 **Fax:** +49-0394825-550

20 Department of Molecular Genetics &

21 Department of Physiology and Cell Biology

22 Leibniz Institute of Plant Genetics and Crop Plant Research (IPK)

23 Gatersleben, Corrensstrasse 3

24 06466 Stadt Seeland, Germany

25

26

27
28 The authors responsible for the distribution of materials integral to the findings presented in
29 this article in accordance with the policy described in the instructions for authors are
30 Hongwen Wang (wangh@ipk-gatersleben.de), Nicolaus von Wirén (vonwiren@ipk-gatersleben.de) and Markus Kuhlmann (Kuhlmann@ipk-gatersleben.de).

31

32

33

34

35

36

37 **Abstract**

38

39 Tiller formation is a key agronomic determinant for grain yield in cereal crops. The
40 modulation of this trait is controlled by transcriptional regulators and plant hormones, tightly
41 regulated by external environmental conditions. While endogenous (genetics) and exogenous
42 (environmental factors) triggers for tiller formation have mostly been investigated separately,
43 it has remained elusive how they are integrated into the developmental program of this trait.
44 The transcription factor *INTERMEDIUM-C (INT-C)*, which is the barley ortholog of the
45 maize domestication gene *TEOSINTE BRANCHEDI (TBI)* has a prominent role in regulating
46 tiller bud outgrowth. Here we show that *INT-C* is expressed in tiller buds, required for bud
47 growth arrest in response to shade. In contrast to wild type plants, *int-c* mutant plants are
48 impaired in their shade response and do not stop tiller production after shading. Gene
49 expression levels of *INT-C* are up-regulated under light-limiting growth conditions, and
50 down-regulated after decapitation. Transcriptome analysis of wild-type and *int-c* buds under
51 control and shading conditions identified target genes of *INT-C* that belong to auxin and
52 gibberellin biosynthesis and signaling pathways. Our study identifies *INT-C* as integrator of
53 the shade response into tiller formation, which is prerequisite for implementing shading
54 responses in the breeding of cereal crops.

55

56 **Key words:** *INTERMEDIUM-C*, yield, barley, bud growth arrest, shade avoidance,
57 decapitation, abscisic acid

58

59

60

61

62

63

64

65

66

67

68

69

70

71 **Introduction**

72

73 Ensuring yield stability of cereal crops is a major requirement for plant breeding in the face of
74 climate change (Kang et al., 2009). In particular, breeding of new elite varieties with
75 optimized shoot architecture, such as tiller number, will allow maintaining high yield
76 potential in unfavorable environments. In many countries, particularly at very high latitudes
77 or on shaded slopes, light is a limiting factor affecting crop growth and yield. Moreover,
78 during the past decades intensive crop management has increased sowing and plant stand
79 densities to improve homogeneity among individual plants that now produce less tillers. To
80 increase light capture, plants have evolved refined mechanisms to maximize light harvesting
81 and/or to prevent shade, i.e. low light intensity and/or a low ratio of red (R) to far-red (FR)
82 light. Suboptimal light triggers a suite of phenotypic changes, defined as the shade avoidance
83 response (SAR) that includes hypocotyl and petiole elongation, an upward orientation of
84 leaves and early flowering. Additionally, a common characteristic of SAR is the suppression
85 of shoot branching in a wide variety of species (Smith and Jordan, 1994; Tucic et al., 2006;
86 Aguilar-Martinez et al., 2007; Gonzalez-Grandio et al., 2013).

87 The extensive work carried out in *Arabidopsis* has provided a detailed understanding of the
88 SAR (Wang and Wang, 2015). By sensing and responding to R and FR light, the five
89 photoreceptors of the phytochrome family (phyA-phyE) regulate a variety of developmental
90 processes (Franklin and Quail, 2010). Among these, phytochrome B (phyB) appears to be the
91 most important photoreceptor involved in shade detection and avoidance (Reed et al., 1993;
92 Ballare, 1999), functioning redundantly with other members of its clade (Stamm and Kumar,
93 2010). Phytochrome proteins act as dimers and exist in two photo-convertible forms: 'Pr' (the
94 red-light-absorbing, inactive form) and 'Pfr' (the far-red-light-absorbing, active form), with
95 the Pfr:Pr ratio reflecting the R:FR ratio of the environment (Smith, 2000). Upon photo-
96 conversion into active Pfr, phytochromes migrate to the nucleus, where they regulate gene
97 expression by interacting with several basic helix-loop-helix (bHLH) transcription factors,
98 including phytochrome interacting factor (PIF) and PIF-like (PIL) proteins (Chen et al., 2004;
99 Duek and Fankhauser, 2005). In many plant species, genome-wide transcriptional dynamics
100 of the SAR have been studied in petioles or leaf blades at the seedling stage, while SAR is
101 less defined in economically important monocots (Devlin et al., 2003; Tao et al., 2008;
102 Hornitschek et al., 2012; Wang et al., 2016).

103 In the agricultural production of graminaceous crop species, plant density is a major
104 determinant for crop yield. Shading caused by elevated plant densities reduces not only
105 photosynthetic active radiation (PAR) flux density but also the R/FR ratio of the light
106 reaching the lower strata of the canopy. Generally, increasing plant density results in
107 progressively stronger suppression of tillering due to accelerated apical shoot development
108 and stem elongation. This pattern continues until the beginning of the stem elongation phase
109 (Zadoks, 1985). Moreover, early-emerging tillers contribute more to grain yield than do tillers
110 that emerge later. The regulation of barley tiller outgrowth by shade has also been supported
111 by the observation that supplemental FR illumination of elongating leaves or of the main stem
112 base reduced the total number of tillers per plant (Skinner and Simmons, 1993). In spite of its
113 great ecological and economic impact, little is known about the underlying molecular
114 mechanisms linking shade-initiated transcriptional changes with the suppression of tiller
115 outgrowth in barley plants, especially regarding the tiller bud that is one of the most important
116 sites of shade action.

117 Lateral shoot growth is coordinately controlled by conserved interactions that regulate the
118 biosynthesis and signaling of the hormones auxin, abscisic acid (ABA), strigolactones (SL),
119 and cytokinins (CK). Auxin and SL, synthesized mainly in the shoot apex and root,
120 respectively, inhibit branching, while CK, synthesized mostly in the root and stem, promote
121 branching (Kebrom et al., 2013; Wang et al., 2018).

122 The class II TEOSINTE BRANCHED1, CYCLOIDEA, and PCF (TCP) transcription factors
123 TEOSINTE BRANCHED 1 (TB1)-like, in monocots, and BRANCHED1 (BRC1)-like, in
124 dicots, act locally inside the axillary bud where they are subject to transcriptional regulation
125 by hormonal cross-talk (auxin-SL-CK) and cause bud growth arrest (Doebley et al., 1997;
126 Aguilar-Martinez et al., 2007; Minakuchi et al., 2010; Martin-Trillo et al., 2011; Braun et al.,
127 2012). Moreover, recent studies have implicated the involvement of TB1 orthologs in the
128 shade-induced response of branch suppression. In *Sorghum bicolor* and maize, active phyB
129 (Pfr) suppresses the expression of the *TBI* gene and induces bud outgrowth. On the other
130 hand, light signals that inactivate phyB allow increased expression of *TBI* and suppression of
131 bud outgrowth (Kebrom et al., 2006; Kebrom et al., 2010; Whipple et al., 2011). In
132 *Arabidopsis*, *BRC1* is upregulated in axillary buds of plants grown at high density and is
133 required for complete branch suppression in these conditions (Aguilar-Martinez et al., 2007).
134 These results suggest that the phytochrome pathway is involved in the control of *TBI* and
135 axillary meristem outgrowth, and provides a link between environmental variation and gene
136 action controlling branching. In barley, *INT-C* is an ortholog of the maize domestication gene

137 *TBI*, and its mutants exhibit higher tiller numbers and enlarged lateral spikelets (Ramsay et
138 al., 2011).

139

140 Here, we investigated the shade avoidance response of early formed tiller buds in barley
141 plants before the rapid stem elongation stage, and studied the role of *INT-C* during the SAR
142 by comparable transcriptome analysis. The analysis revealed that the dynamics of *INT-C*
143 expression during SAR is critical for genome-wide reprogramming of gene expression and
144 that the gene categories affected support a central role of *INT-C* in tiller bud arrest. A
145 comparison of genes responding to shade-induced bud arrest and decapitation-triggered bud
146 activation allowed us to identify key regulators influencing *bud dormancy* and *bud activation*
147 genes. Thus, these findings would enable us to better understand the genetic mechanisms
148 controlling the reversible transition of growth to dormancy in barley tiller buds.

149

150 **Materials and Methods**

151

152 **Plant material and growth conditions.** *Hordeum vulgare* cv. Bowman, a two-rowed spring
153 barley cultivar, was used as wild type for comparison to its near isogenic mutant BW421 (*int-*
154 *c.5*) (Ramsay et al., 2011). For the experimental analyses except the shading experiment, wild
155 type and *int-c* mutant plants were cultivated in a greenhouse. Seeds were sown in either 54 or
156 96 well trays and germinated in a climate chamber for 10 days at 11°C day and 7°C night
157 temperature under 16 h light. After that, seedlings were transferred to pots (diameter 16 cm)
158 filled with 2 parts of compost, 2 parts of “Substrat 2” (Klasmann) and 1 part of quartz sand,
159 and allowed to grow in the greenhouse at 20°C day/14°C night under 16 h light. For the
160 density experiments, three barley planting densities (1, 5, 10 plants pot⁻¹) were established in
161 pots (size: 21-liter, top diameter: 310 cm, base diameter: 250 cm, height: 214 cm), and the
162 planting density test was repeated four times. For the decapitation experiments, when plants
163 were grown till the early stem elongation stage, the shoot apices were removed, and the apical
164 dominance test was repeated three times. For the shading experiments, seedlings were grown
165 in a climate-controlled growth chamber at a temperature of 12°C, 70% humidity and a 12/12 h
166 day/night cycle. Green shading was achieved by using a green plastic filter (122 Fern Green;
167 LEE Filters, Andover, UK) (Kegge et al., 2013).

168

169 **Sequence retrieval for TCP proteins.** In order to identify barley genes putatively encoding
170 TCP transcription factors, the latest barley annotation and genome sequence at

171 <http://webblast.ipk-gatersleben.de/barley/viroblast.php> was searched using the TBLASTN
172 algorithm with Arabidopsis TCP proteins or TCP domains as query sequence. All redundant
173 sequences were discarded from further analysis based on ClusterW (Thompson et al., 1994).
174 Furthermore, to verify the reliability of the initial results, all non-redundant candidate TCP
175 sequences were analyzed to confirm the presence of the conserved TCP domain using the
176 InterproScan program (Quevillon et al., 2005). The sequences of TCP family members in the
177 genome of Arabidopsis were retrieved from the PlantTFDB plant transcription factor database
178 (<http://planttfdb.cbi.pku.edu.cn/>, v3.0). As for *Antirrhinum majus* and *Oryza sativa* TCP
179 sequences, they were obtained from NCBI.

180

181 **Phylogenetic analysis.** Multiple sequence alignments were conducted on the amino acid
182 sequences of TCP proteins in Arabidopsis and barley genomes using Cluster X (Thompson et
183 al., 1997) with default settings. Subsequently, MEGA 6.0 software (Tamura et al., 2013) was
184 employed to construct an unrooted phylogenetic tree based on alignments using the Neighbor-
185 Joining (NJ) method with the following parameters: JTT model, pairwise gap deletion and
186 1,000 bootstraps.

187

188 **Extraction and quantification of ABA.** ABA was extracted from fresh plant materials using
189 ethyl acetate (100%). Isotopically labelled D6-ABA was used as an internal standard and
190 added to each sample during the extraction procedure. Extraction was carried out twice with 1
191 ml of ethyl acetate at 4°C. The supernatant collected after centrifugation (13.000 g, 10 min,
192 and 4°C) was evaporated to dryness at room temperature using a vacuum concentrator. The
193 dried samples were dissolved in acetonitrile: methanol (1:1) and filtered using a 0.8 µm filter
194 (Vivaclear). The filtrate (10 µL) was used for subsequent quantification by LC-MS/MS
195 (Dionex Summit coupled to Varian 1200 L). Chromatographic separation was carried out on a
196 C18 column (4 µm, 100 mm; GENESIS; Vydac/USA). MRM and quantification was done
197 using the mass traces 263/153 for ABA and 269/159 for D6-ABA. The validity of the
198 extraction and measurement procedure was verified in recovery experiments (approx. 82-
199 95%). Quantification was based on calibration with known ABA standards and individual
200 recovery rates for the samples, as described in (Kong et al., 2008).

201

202 **qRT-PCR and microarray hybridization & data analyses.** RNA was extracted from fresh
203 plant tissues from independent or pooled biological replicates with the same treatment using a
204 plant mini RNA kit (Qiagen, Hilden, Germany) following the manufacturer's protocol, and its

205 quality and quantity assessed with a Nano drop device (Peqlab, Erlangen, Germany). A 500-
206 ng aliquot was taken as template for the synthesis of the first cDNA strand, primed by
207 oligo(dT), using a RevertAid cDNA kit (ThermoFisher SCIENTIFIC, Waltham, MA, USA).
208 The subsequent qRT-PCR was based on the Power SYBR[®] Green PCR Master Mix
209 (ThermoFisher SCIENTIFIC) and conducted in an Applied Biosystems 7900HT Fast Real-
210 Time PCR system (ThermoFisher SCIENTIFIC) following the manufacturer's protocol.
211 Relative transcript abundances were obtained using $\Delta\Delta C_T$ method (Livak and Schmittgen,
212 2001) and were normalized against the abundance of serine/threonine phosphatase PP2A
213 transcript. The primer sequences employed are given in Supplemental Table S6. The presence
214 of a unique PCR product was verified by dissociation analysis and each qRT-PCR was
215 repeated at least three times. Each biological replicate was represented by three technical
216 replicates.

217 For the microarray procedure, the same RNA samples extracted from three biological
218 replicates was used and the quality of the RNA was verified with a Bioanalyzer 2100 device
219 (Agilent Technologies, Santa Clara, CA, USA). The RNA was labeled by using the Low input
220 QuickAmp Labeling kit (Agilent Technologies) and hybridized, following the manufacturer's
221 protocol, to a custom-synthesized 60 k Barley Microarray (Agilent Technologies) (Koppolu et
222 al., 2013). The resulting data were analysed using GeneSpring 13.0 GX software (Agilent
223 Technologies). After quantile normalization and baseline transformation to the median of all
224 samples, the probesets (genes) were filtered by Coefficient of Variation <50%, followed by
225 moderated T-Test and Bonferroni-Holm multiple testing corrections. Probesets passing the P-
226 value cut-off <0.05 with a fold change of ≥ 2.0 were selected as differentially expressed genes
227 (DEG). Analyses of functional categories with *INT-C*-dependent upregulated and
228 downregulated genes were performed using MapMan. The fold enrichment was calculated as
229 follows: (number in class input_set/number of total input_set)/ (number in class reference_set/
230 number of total reference_set). The *P* value was determined by a hypergeometric distribution
231 test (R Core Team, 2013). The data was sorted by fold enrichment with a cut-off of $P < 0.05$.
232 For the specific pathway enrichment analysis by Wilcoxon-Rank-Sum test was implemented
233 in MapMan. The resulting enrichments for the functional classes ($p < 0.05$, determined by a
234 hypergeometric test; R Core Team, 2013) provided a map of gene modules regulated in
235 dependence of *INT-C* during SAR. To confirm that the common genes of the two identified
236 groups are not by random, the test of statistical significance was applied by a web-based tool
237 at http://nemates.org/MA/progs/overlap_stats.html. The co-regulated genes were retrieved

238 from Genevestigator (Zimmermann et al., 2004), and Gene Ontology analysis was performed
239 in agriGO v2.0 with default parameters (Tian et al., 2017).

240

241 **Statistical analysis.** To test the statistical significance of the data, Student's *t* test and one-
242 way analysis of variance (ANOVA) with Tukey test for significance were used. Asterisks
243 denote significant differences in Student's *t* tests. Different letters denote significant
244 differences in Tukey's test.

245

246 **Results**

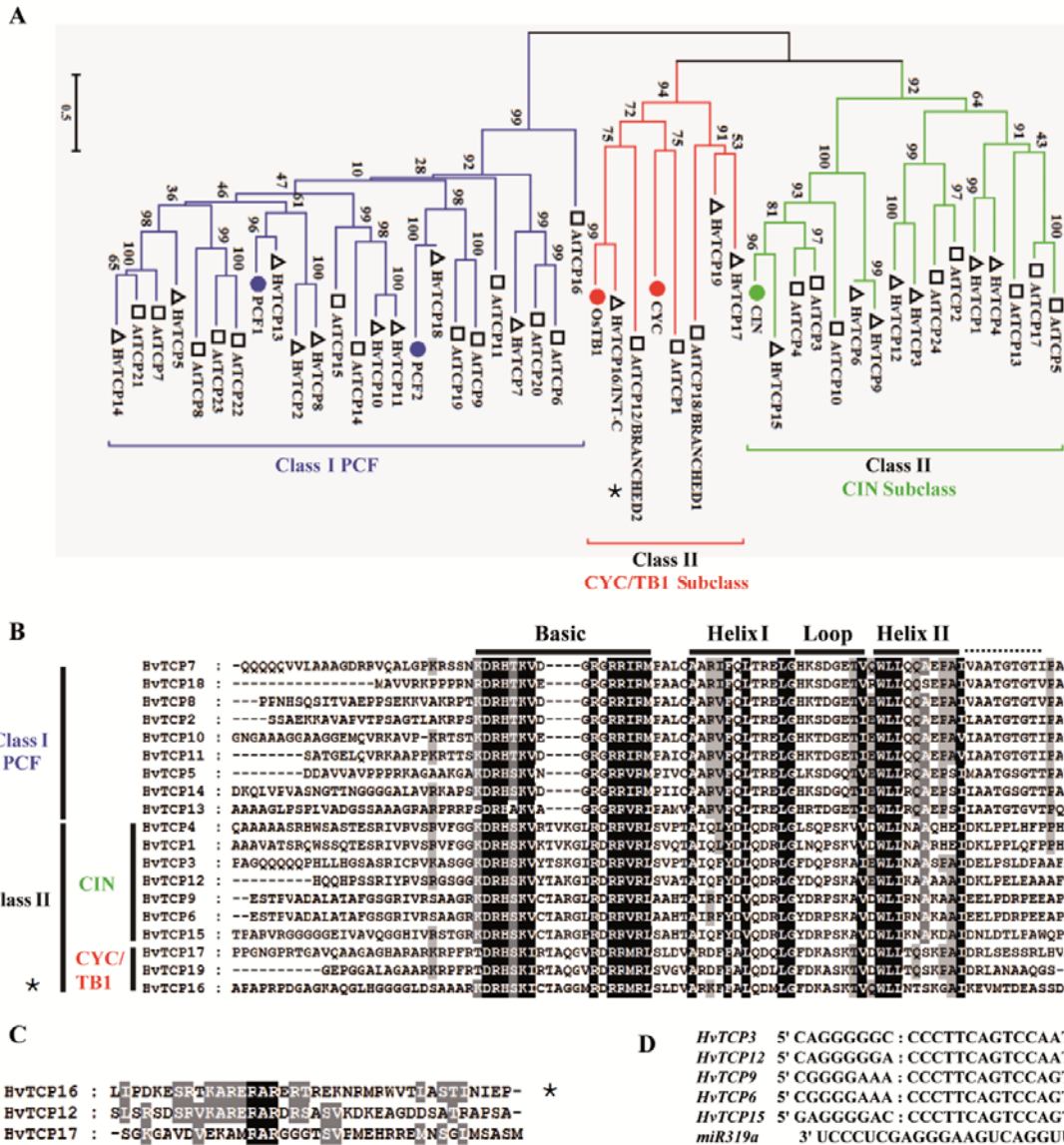
247

248 ***INT-C* is a member of the barley TCP gene family**

249 *INTERMEDIUM-C* (*INT-C*) is the barley orthologue of *TEOSINTE BRANCHED1* (Ramsay
250 et al., 2011), one of the name giving members of the well-studied *TEOSINTE BRANCHED1*,
251 *CYCLOIDEA*, *PROLIFERATING CELL NUCLEAR ANTIGEN BINDING FACTOR*
252 (TCP) gene family (Li, 2015). TCP transcription factors are defined by the TCP domain,
253 which is a 59 aa- long basic helix-loop-helix (bHLH) structure which provides the ability to
254 bind GC-rich DNA sequence motifs (Martin-Trillo and Cubas, 2010). In barley, *INT-C* is
255 encoded by *HORVU4Hr1G007040* and was identified as corresponding gene of the *vrs5* locus
256 on chromosome 4 (Ramsay et al., 2011) being involved in the fertility of lateral spikelets.

257 To identify the genes closest to *INT-C*, the barley TCP gene family was analyzed using the
258 latest barley annotation and genome sequence at [http://webblast.ipk-](http://webblast.ipk-gatersleben.de/barley/viroblast.php)
259 [gatersleben.de/barley/viroblast.php](http://webblast.ipk-gatersleben.de/barley/viroblast.php) and the TBLASTN algorithm with Arabidopsis TCP
260 proteins or TCP domains as query sequence (Figure 1A; Supplemental Table S1). This family
261 consists of 20 genes which contain a putative TCP-helix-loop-helix-type domain at the N-
262 terminus (Figure 1B). The phylogenetic tree which was built based on multiple alignments of
263 the TCP domain in TCP proteins showed that barley TCP proteins could be divided into two
264 groups, as for all species so far (Figure 1A/B). The class I group was formed by nine
265 predicted proteins related to the PCF rice factors (Kosugi and Ohashi, 1997), while class II
266 was comprised of eleven predicted proteins related to the *Antirrhinum* *CYC* and *CIN* genes
267 and to *OsTBI* (Luo et al., 1996; Doebley et al., 1997; Nath et al., 2003; Takeda et al., 2003).
268 In addition, the class II group could be further divided into two subclades: the *CIN* group
269 formed by eight members and the *CYC/TB1* group formed by three members. *HvTC16* and
270 *HvTC17* from the class II *CYC/TB1* contain an R domain that is also found in *HvTC12* from
271 the class II *CIN* group (Figure 1C), as previously described in Arabidopsis (Yao et al., 2007).

272 Although in eudicots several CYC/TB1 sequences are found, and phylogenetic analyses have
273 suggested that duplications within this clade occurred at the base of eudicots, in monocots
274 only one type of CYC/TB1 has been identified (e.g., *OsTB1*) (Howarth and Donoghue, 2006).
275 Our phylogenetic analysis revealed that, based on the absence of the R domain, none of the
276 newly identified barley TCP genes can be considered as paralogue of *INT-C*.
277 As described for the model plant Arabidopsis, five of the CIN subclade members are post-
278 transcriptionally regulated by *miRNA319* (*AtTCP2*, *3*, *4*, *10* and *24*) (Palatnik et al., 2003; Ori
279 et al., 2007; Palatnik et al., 2007). In barley *hvu-miR319a*
280 (UUGGACUGAAGGGAGCUCCC) is encoded by CL16998_Contig1 (Ozhuner et al., 2013)
281 and expressed in roots, while it is not detectable in leaf tissue. The closest barley homologs of
282 these Arabidopsis genes are the five genes, *HvTCP3*, *HvTCP6*, *HvTCP9*, *HvTCP12*, and
283 *HvTCP15*. These barley CIN subclade members contain sequences with putative binding sites
284 for *hvu-miR319* (Supplemental Table S1). Figure 1D shows the alignment of the target sites of
285 these genes with the *miR319* sequence. This suggests that regulation of leaf development by a
286 redundant set of miRNA-regulated homologous TCP genes occurs in barley, while *INT-C*
287 does not represent a miR319 target.
288



289

290 **Figure 1 Phylogenetic relations of Arabidopsis and barley TCP proteins.** A) The phylogenetic tree of TCP
 291 proteins was built based on multiple alignment of the TCP domain amino acid sequence using the Neighbor-
 292 Joining method with 1000 bootstrap replicates. Blue, red and green lines indicate the PCF, CYC/TB1 and CIN
 293 clades, respectively. Each Arabidopsis protein is indicated by a square, each barley protein is indicated by a
 294 triangle. B) Alignment of the TCP domain and adjoining sequence for the predicted barley TCP proteins. Overall
 295 conserved amino acids are shaded in black. Amino acids 80% or 100% conserved in Class II or Class I are
 296 shaded in light gray and dark gray, respectively. The Basic, Helix I, Loop, and Helix II regions are indicated. C)
 297 Alignment of the R-domain of Class II subfamily members. Amino acids are expressed in the standard single
 298 letter code. Sequences were aligned with ClustalW and represented with Genedoc. D) Alignment of putative
 299 target areas for *miR319* (aligned in reverse). *INT-C* (*HvTCP16*): asterisks

300

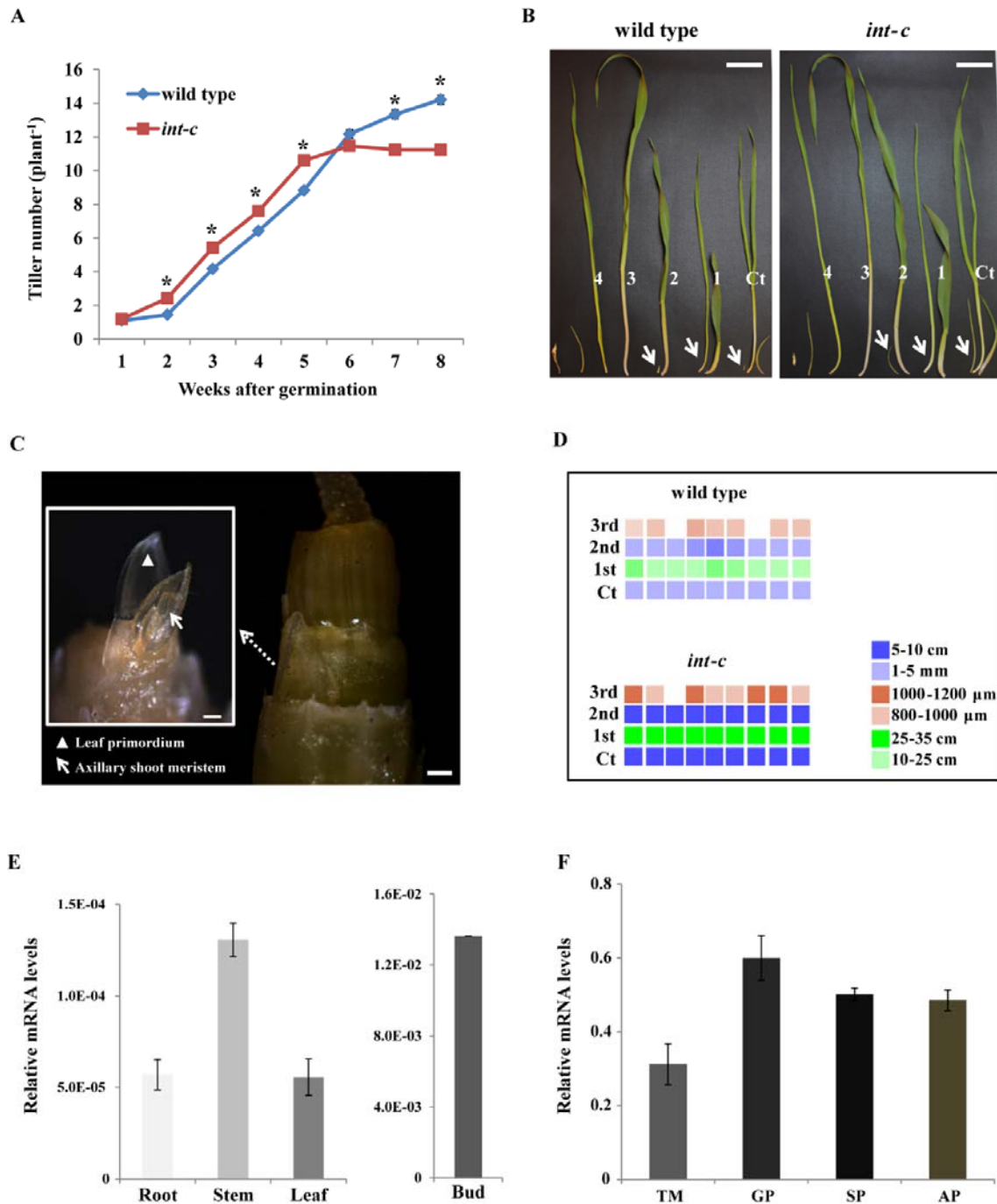
301 ***INT-C* loss-of-function leads to an early promotion of tiller bud outgrowth in barley**

302 Previous studies noticed that *int-c* mutants in various cultivars produce more tillers than the
 303 respective wild type plants during early vegetative stages (Ramsay et al., 2011; Liller et al.,
 304 2015). However, this increased tiller formation did not translate into more productive tillers.
 305 In contrast the number of tillers was significantly lower at the point of harvest. The growth

306 experiment described here performed with the near isogenic mutant BW421 (*int-c.5*) and the
307 corresponding wild type confirmed these earlier observations. An increase in tiller number in
308 *int-c* was only detectable at the early developmental stages (Figure 2A) between two and five
309 weeks after germination. At later developmental stages (6 to 8 weeks after germination), the
310 pattern of tiller number was reversed. This observation correlated with an earlier anthesis of
311 *int-c* compared to the wild type cv. Bowman (Supplementary Figure 1), leading to an earlier
312 arrest of tiller bud production in *int-c*. The tillers of barley are formed in a sequential order,
313 starting with the first tiller bud under the coleoptile. The development of the tiller buds in the
314 axils of successive leaves was studied by dissecting the plants at different developmental
315 stages (Figure 2B). To investigate the involvement of *INT-C* in bud initiation and bud
316 outgrowth, the primary tiller buds were classified (Figure 2C/D) as dormant bud (800~1200
317 μm), outgrowing bud (1.5~100 mm) or tiller emergence (10~35 cm) in each leaf axil at an
318 early developmental stage (2 to 3 weeks after germination). Figure 2D indicates the enhanced
319 bud outgrowth in *int-c* mutants compared to the wild type. This result suggests that the
320 outgrowth of tiller buds is accelerated in *int-c* mutants at early developmental stages but is
321 slowed down at later stages (> 5 weeks).

322 *INT-C* mRNA levels were analyzed by real-time qRT-PCR in different tissues and during
323 spike development (Figure 2E/F). *INT-C* mRNA was detectable at highest levels in tiller buds,
324 supporting its role in the control of tiller bud development. It was expressed at lower levels in
325 other tissues such as root, stem and leaf. During spike meristem development mRNA levels of
326 *INT-C* peaked at the glume primordium stage. In the later stages (stamen primordium and awn
327 primordium) relative high levels of *INT-C* mRNA were persisting. This peak of expression
328 correlated with the observation that after awn primordium stage profound differences in the
329 development of lateral spikelet in *int-c* occurred compared to wild type (Ramsay et al., 2011).

330



331

332 **Figure 2. *INT-C* is involved in barley plant architecture by tiller bud outgrowth.** Analysis of tiller
 333 development in wild type and *int-c* plants. **A)** Tiller number of *int-c* and wild type plants 1-8 weeks after
 334 germination ($n = 25-30$ plants). Asterisks indicate significant differences (Student's t test, $P < 0.001$) between
 335 wild type and *int-c* mutant plants. **B)** Dissected tillers from successive leaf axils in about 2 to 3-week-old
 336 seedlings. Ct, coleoptile tiller; 1-4, order of leaves; bars = 5 cm; arrows, tiller buds. **C)** Exemplary tiller bud
 337 formation stage in the third leaf axil. The area of the close-up view is outlined with a white box in the left image.
 338 Dissection of a tiller bud at this stage will reveal a shoot apex with leaf primordia and meristematic dome. Scale
 339 bars represent 200 μm . **D)** Schematic representations of tiller bud production in each leaf axil of the wild type
 340 and *int-c* in 2- to 3-week-old seedlings. Each column stands for a single plant, and each row stands for a leaf axil
 341 in order from bottom to top, starting with the coleoptile tiller. Different color squares denote different tiller bud
 342 lengths.

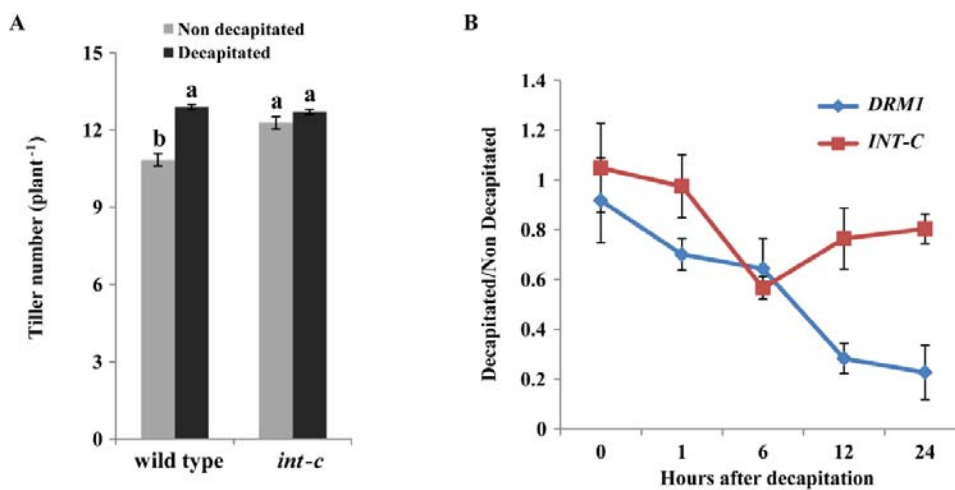
343 **E)** *INT-C* (HvTCP16) mRNA levels in different tissues and **F)** during spike development as analyzed by real-
 344 time qRT-PCR. Bars represent means \pm SD; $n = 3$ biological replicates. Serine/threonine protein phosphatase

345 HvPP2A-4 mRNA was used as a reference. TM, triple mound; GP, glume primordium; SP, stamen primordium;
346 AP, awn primordium.

347

348 ***INT-C* mRNA abundance decreased after decapitation**

349 Apical dominance is the inhibitory control exerted by the shoot apex over the outgrowth of
350 the lateral buds (Cline, 1997). Decapitation stimulates bud reactivation after breaking the
351 apical dominance (Hall and Hillman, 1975; Napoli et al., 1999; Cline, 2000; Tatematsu et al.,
352 2005; Aguilar-Martinez et al., 2007). To analyze the involvement of *INT-C* in integrating the
353 decapitation response into bud outgrowth we compared barley *int-c* mutant plants to the
354 respective wild type plants. For this approach, three-week-old plants that had undergone early
355 stem elongation, were decapitated. Two weeks later, two tiller buds of decapitated Bowman
356 plants had elongated prematurely. Thus, total tiller number in decapitated wild-type plants
357 reached the same level as in *int-c* mutants, in which decapitation had no effect (Figure 3A).
358 To investigate whether this response was related with a transcriptional downregulation of
359 *INT-C*, mRNA levels in axillary buds were analyzed by real time qRT-PCR after decapitation,
360 before any visible sign of bud outgrowth (Figure 3B). *INT-C* mRNA decreased significantly 6
361 h after decapitation. *DRMI/ARP* (*DORMANCY-ASSOCIATED GENE/AUXIN-REPRESSED*
362 *PROTEIN*) mRNA, an early marker for bud dormancy (Stafstrom et al., 1998; Tatematsu et
363 al., 2005), also showed reduction and reached its minimum 24 h after decapitation. These
364 results support the idea that *INT-C* is involved in the early response to bud release from apical
365 dominance and required for bud activation.



366 **Figure 3. *INT-C* expression in response to decapitation.** A) Tiller number of cv. Bowman (wild type) and *int-c*
367 plants 2 weeks after decapitation. Bars represent means \pm SD; $n = 3$ replicates with ≥ 16 plants. Different letters
368 indicate significant differences according to Tukey's test ($P < 0.05$). B) Ratio of mRNA levels of *INT-C* and
369 *DRMI* in tiller buds between decapitated and non-decapitated plants. Relative mRNA abundance of *INT-C*
370 mRNA was analyzed by real-time q-RT-PCR. Bars represent means \pm SD; $n = 4$ biological replicates.
371

372 *Serine/threonine protein phosphatase HvPP2A-4* was used as a reference gene. Analyzed is the early
373 transcriptional response within 24 hours after decapitation.

374

375 **Transcriptome analysis of buds after decapitation**

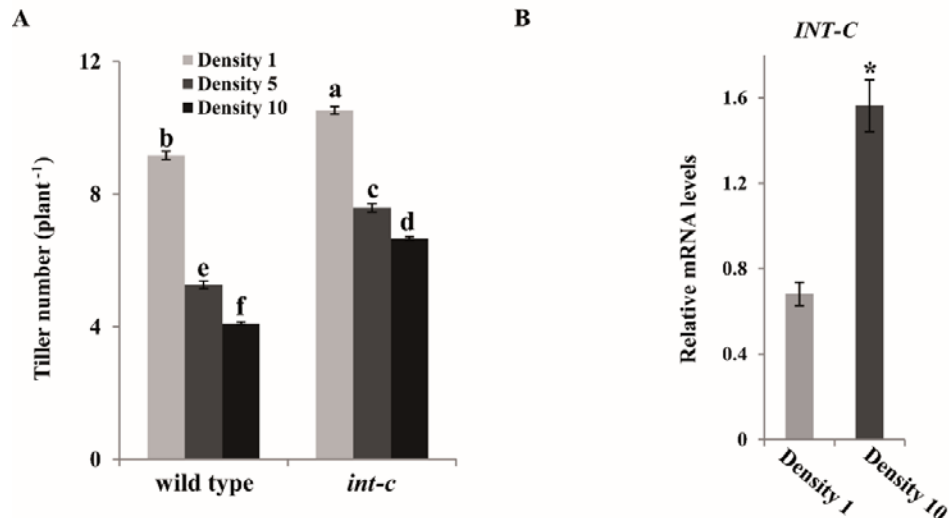
376 To investigate the transcriptome response of dormant versus activated buds, Agilent 8 × 60K
377 customized barley microarray expression analysis (Thirulogachandar et al., 2017) using total
378 mRNA prepared from tiller buds at the early stem elongation stage was performed. The time
379 point 24 h after decapitation was chosen for the following two reasons: 1) down-regulation of
380 *DRM1* expression was evident at this time point (Figure 3B) and 2) this time point was one
381 day before the first visible effects of decapitation on the growth were detectable (2 d after
382 decapitation, Figure 3A).

383 1704 differential expressed genes (DEGs) were detected in tiller buds of decapitated versus
384 non-decapitated plants (Supplementary Table S2), among those 1011 were down-regulated
385 and 693 up-regulated. Microarray results were confirmed by qRT-PCR for selected genes
386 (Supplemental Figure 2). Besides *DRM1*, which was found among the down-regulated genes,
387 several genes encoding transcription regulators were detected. 81 out of 494 DEGs regulated
388 in opposite direction under shading conditions could be mapped to the term transcription
389 regulator Associated with the term ABA are the auxin binding protein ABP44 and a putative
390 ripening related bZIP Protein (CAB85632). The class of AP2-EREBP transcription regulators
391 was found to be down regulated upon decapitation. The up-regulated genes included a large
392 number of ribosomal proteins, cell organization, and cell cycle-related genes.

393

394 **Plant density affects *INT-C* expression**

395 Planting density affects shoot branching in many plant species. Low plant density results in
396 more branches, compared to growth in dense plant stands as a result of a neighbor-sensing
397 response (Casal et al., 1986). To test the impact of plant density on *INT-C*, wild type and *int-c*
398 plants were grown in three different densities under greenhouse conditions (1, 5 and 10 plants
399 per pot). Tiller numbers were counted until the early stem elongation stage (Figure 4).



400

401 **Figure 4. *INT-C* expression responds to planting density.** A) Tiller number of wild type and *int-c* plants
402 grown at planting densities of 1, 5, or 10 plants per pot. Plants were analyzed 5 weeks after sowing. Bars
403 represent means \pm SD; $n = 3$ replicates with ≥ 20 plants. Different letters indicate significant differences
404 according to Tukey's test ($P < 0.01$). B) Transcript levels of *INT-C* in the tiller bud tissue analyzed by real-time
405 PCR at a density of 1 or 10 plants per pot. Bars represent means \pm SD; $n = 3$ biological replicates.
406 *Serine/threonine protein phosphatase HvPP2A-4* was used as a reference gene. Asterisk indicates significant
407 difference according to Student's *t* test at $*P < 0.001$.

408

409 Wild-type plants responded to increased planting density with reduced tillering. At a density
410 of ten plants per pot, tiller bud suppression was more than half, as tiller number was 56%
411 lower than in plants grown at one plant per pot. However, *int-c* mutants showed reduced
412 sensitivity to this condition (33% reduction compared with plants at one plant per pot). The
413 mRNA levels of *INT-C* were then analyzed by RT-qPCR in wild type plants grown at low
414 (one plant per pot) and high (ten plants per pot) density. At high density, *INT-C* mRNA levels
415 showed a two-fold increase compared to those at low density (Figure 4B). These results
416 support the involvement of transcriptional regulation of *INT-C* on bud dormancy.

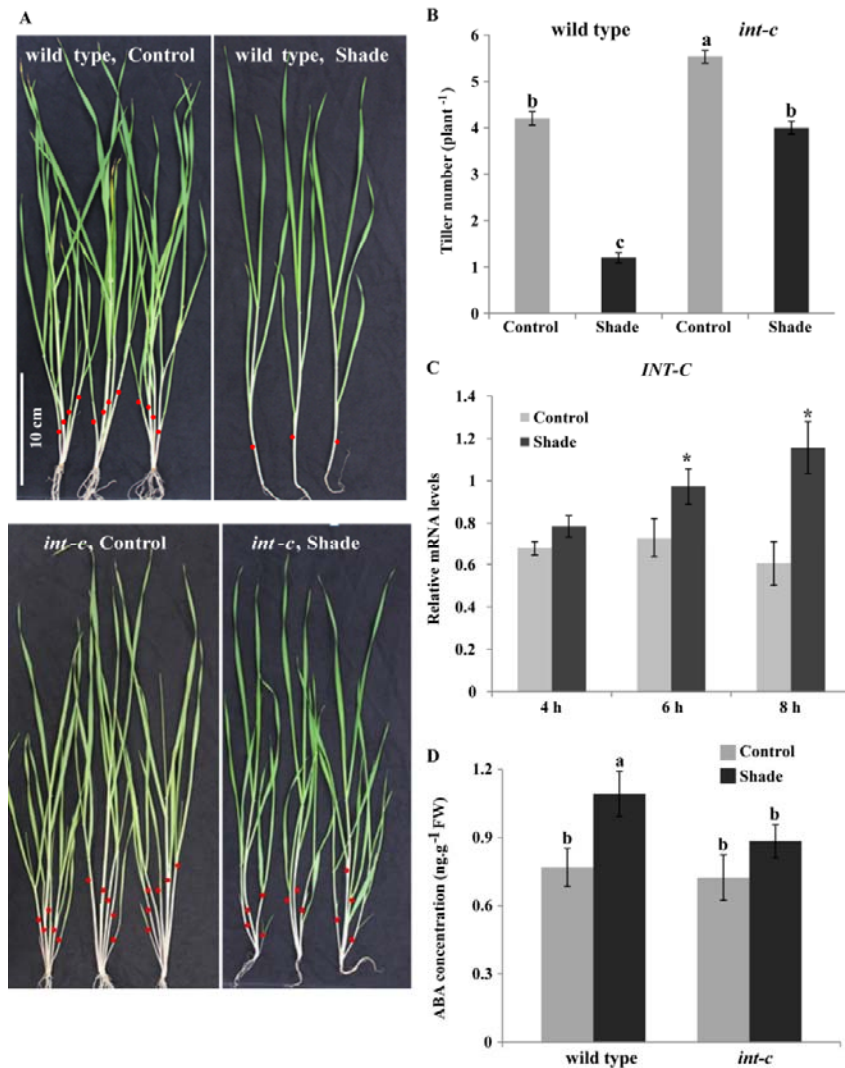
417

418 ***INT-C* is upregulated as part of the shade avoidance response**

419 To further examine whether *INT-C* is participating in the shade avoidance response, plants
420 were grown under two different light conditions: control light (PAR: $840 \mu\text{mol m}^{-2} \text{s}^{-1}$; R:FR
421 ratio = 2.2), and low R:FR light mimicking shade imposition by neighboring plants (green
422 shade, PAR: $260 \mu\text{mol m}^{-2} \text{s}^{-1}$; R:FR ratio = 0.2) (Kegge et al., 2013). To minimize a putative
423 bias resulting from variations in leaf number and *int-c* mediated earlier flowering, plants were
424 grown at conditions attenuating the *int-c* early flowering phenotype (Figure 5A).

425 The shading treatment was started at the two-leaf stage. Four weeks later primary tiller
426 number was quantified. Bowman plants grown under shade conditions responded strongly and

427 had 4 times less tillers than plants grown in control conditions (Figure 5B), indicating that
428 exposure of plants with young vegetative buds to a low R:FR ratio promotes bud arrest in
429 barley. In contrast, the response of *int-c* mutants to shading was much weaker. *int-c* plants
430 grown under shade had only 1.4 times fewer tillers than plants grown under normal light
431 conditions (Figure 5A/B). Other phenotypic shade avoidance responses, such as hyponasty
432 and stem elongation, were indistinguishable between the wild type and mutant plants (Figure
433 5A). The short-term response of *INT-C* to shade treatment was analyzed by transferring plants
434 at the five-leaf stage (when plants had small vegetative buds) to low R:FR light. The mRNA
435 levels of *INT-C* in tiller buds increased after 4, 6 or 8 h exposure to shade, indicating a
436 transcriptional activation of *INT-C* in response to shade (Figure 5C). This result is in
437 agreement with the increase of tillers in plants grown in dense stands. The higher tiller
438 number in *int-c* coincided with a lower concentration of ABA in tiller buds (Figure 5B, D),
439 supporting the role of ABA as mediator of *INT-C*-dependent tiller bud suppression in the
440 shade.



441

442 **Figure 5. Effect of shading on tiller bud outgrowth and *INT-C* expression.** A) Tillering phenotype of wild-
 443 type and *int-c* plants grown under control conditions or shading. Red dots indicate the primary tillers. B) Tiller
 444 number of wild type and *int-c* plants grown under control or shade conditions. Bars represent means \pm SD; Three
 445 independent experiments with $n \geq 35$ plants each. Different letters indicate significant differences according to
 446 Tukey's test ($P < 0.01$). C) Transcript levels of *INT-C* analyzed by qPCR, in buds of shaded plants, relative to
 447 levels in control plants. Bars represent means \pm SD; $n = 3$ biological replicates. *Serine/threonine protein*
 448 *phosphatase PP2A-4* was used as a reference gene. Asterisk indicates significant difference according to
 449 Student's *t* test at $*P < 0.05$. D) ABA concentrations in tiller buds of wild type and *int-c* plants 6 h after exposure
 450 to shade. Bars represent means \pm SD of six independent biological replicates. FW: Fresh Weight. Different
 451 letters indicate significant differences according to Tukey's test ($P < 0.05$).

452

453 Transcriptome analysis of tiller buds after shading identifies *INT-C* dependent genes

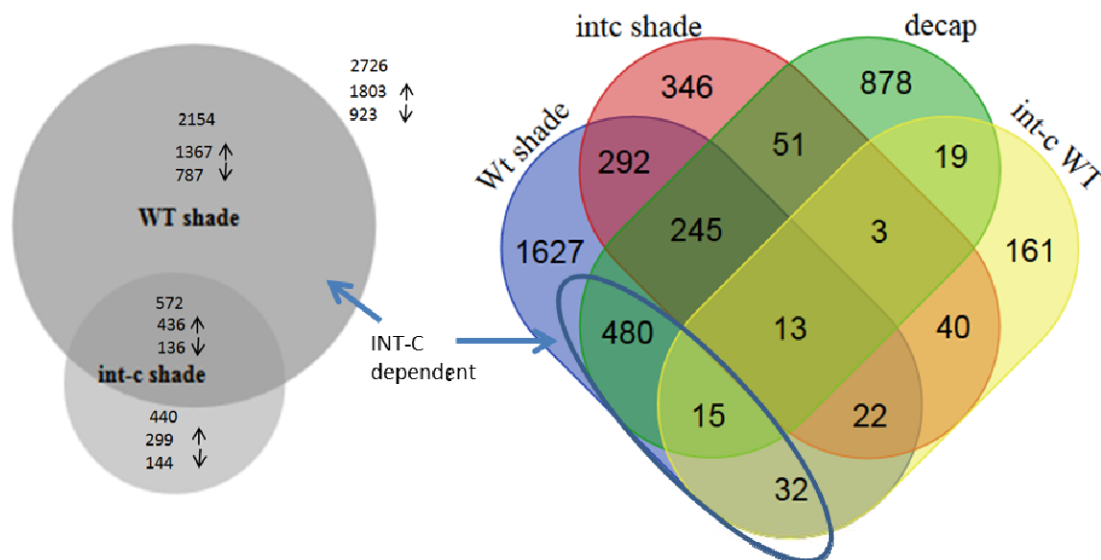
454 To get further insight into the molecular mechanisms of *INT-C*-mediated growth responses,
 455 the transcriptome of tiller buds in wild type and *int-c* plants was analyzed. The plants were
 456 exposed to control conditions or shade (Figure 5) and the transcriptome was analyzed 6 h after
 457 exposure to shade using an Agilent $8 \times 60K$ customized barley microarray. As *INT-C*

458 expression was highest in buds (Figure 1), we selected this tissue for detailed analysis of RNA
459 extraction.

460 While under control conditions a minor influence of *int-c*-dependent transcript changes was
461 found, 305 differentially expressed genes (DEGs) were identified between WT vs *int-c*, out of
462 which 185 were up- and 120 down-regulated. Under shading a stronger effect of *int-c* on the
463 transcriptome was noted. In wild type buds, 2726 shade-responsive DEGs (1803 DEG up- and
464 923 DEGs down-regulated) were detected. In the *int-c* mutant, a total of 906 DEGs were
465 identified in response to shade with 226 up-regulated genes and 680 down-regulated genes
466 (Figure 6, Supplemental Table S2). DEGs detected by microarray were validated and
467 confirmed for five upregulated and five downregulated genes by qRT-PCR (Supplementary
468 Figure 3). The number of DEGs in response to shading decreased by ~67% in *int-c* (Figure 6,
469 Supplemental Table S2). This drop supports the hypothesis of the involvement of *INT-C* in
470 the shade response. The overlapping DEGs, detectable in wild type and *int-c* are related to a
471 common shade avoidance response independent of *INT-C*, while DEGs detectable in the wild
472 type could directly or indirectly depend on *INT-C* function. These 2154 DEGs were termed
473 *INT-C*-dependent genes of the shade response (Figure 6, Supplemental Table S2).

474

475



476

477 **Figure 6.** Venn diagram of differentially expressed genes (DEGs) detected after shade treatment in cv. Bowman
478 wild type (Wt shade) and *int-c* (*int-c* shade). These blocks were compared to DEGs detectable after decapitation
479 (decap) and *int-c* mutant and wild type (*int-c* versus WT). Numbers indicate transcript changes of fold-change \geq

480 2 at an FDR of $p < 0.05$. (shade: INT-C mRNA induced, int-c: no functional INT-C, decap: INT-C mRNA
481 reduced).

482

483 In Bowman buds, the upregulation of *INT-C* after shading (2.56-fold increase at an FDR of
484 $4.78E-04$ could be confirmed. In the BW421 (*int-c.5*) deletion mutant a similar induction of
485 *INT-C* (2.10-fold increase, FDR = 0.0086) was detectable (Supplementary Table S2).
486 However, in the *int-c.5* mutant the deletion in the *INT-C* gene leads to a frameshift in the C-
487 terminus downstream of the R-domain. This mutation leads to a nonfunctional gene product.

488 The inspection of the respective marker genes *HAT4/ATHB2*, *PIF3* and *PIF4* (Leivar and
489 Monte, 2014) by their transcriptional activation validated the applied experimental shade
490 conditions (Supplementary Table S2). Among the significantly upregulated genes after shade
491 in the wild type, transcript levels of the marker gene *DRMI* that is associated with tiller bud
492 dormancy (Stafstrom et al., 1998; Tatematsu et al., 2005) were found to be more than two-
493 fold higher (Supplementary Table S2).

494 As shown in Figure 5A the shade response led to a transcriptional activation of *INT-C* and a
495 repression of tiller outgrowth. In contrast, the decapitation of barley plants resulted in a
496 reduced expression of *INT-C* and the opposite phenotype. As *INT-C* expression was reduced
497 under this simulated condition, the generated dataset was used to validate the list of *INT-C*-
498 dependent shade response genes (Supplementary Table S2).

499 The Venn diagram (Figure 6) illustrates 753 overlapping DEGs after decapitation and after
500 shading (27% of 2726 DEGs after shading and 44% of 1704 DEGs after decapitation). 495
501 (29%) of the decapitation-induced DEGs were also detectable in response to shading. Almost
502 all of these DEGs were oppositely regulated after decapitation and shading, respectively
503 (Supplementary table S3). This list was defined as INT-C dependent genes.

504 MapMan software was used to define gene functional categories (Thimm et al., 2004; Usadel
505 et al., 2005). For the *INT-C* dependent genes we identified hormone- and stress-related genes
506 among the upregulated genes and cell division- and protein synthesis-related genes among the
507 downregulated genes as the most prominent functional categories.

508 As all INT-C-dependent genes showed opposite responses after decapitation and under shade,
509 these gene sets infer the causal mechanisms associated with bud activation and bud arrest,
510 respectively. 123 genes (25 %) found to be upregulated after decapitation were
511 downregulated under shade while 372 (75 %) genes downregulated after decapitation were
512 upregulated under shade (Figure 6; Supplementary Table S3). During decapitation-induced
513 bud activation, *INT-C* was rapidly downregulated (Figure 3B). Further, a strong overlap of
514 DEGs responding to decapitation and shading was observed. Theoretically, the 372

515 downregulated (after decapitation) genes might be directly involved in the promotion of
516 axillary bud arrest. This group included a number of genes related to ethylene, abscisic acid,
517 auxin, and gibberellin signaling (AP2/ERBP, ACC, ERF1, IAA17, and GID1L2), as well as
518 protein degradation (SKIP1, SKIP5, SKP2A, UBQ3 and UBQ4). Moreover, genes related to
519 sugar metabolism and transport also identified within that group (TPS6, sucrose transporter).
520 Trehalose-6-phosphate is known to be involved in sugar signaling (Figuroa and Lunn, 2016).
521 On the other hand, the 123 upregulated genes (after decapitation) could be involved in
522 promoting axillary bud growth. This group included many genes associated with chloroplast
523 function and chlorophyll synthesis (chlorophyll binding protein, ATP synthase), protein
524 synthesis (EF-Ts, ribosomal protein), and chromatin structure (HISTONE H3.2, HISTONE
525 2B. 3). This set of genes was co-regulated with a subset of genes related to functional
526 categories involved in thylakoid and photosynthesis (Supplementary Figure 4).

527

528 **Discussion**

529

530 The present study shows that *INT-C* is transcriptionally regulated by apical dominance and by
531 light perception and that *INT-C* expression in tiller buds regulates tillering in response to these
532 signals. This highlights the role of *INT-C* as a major transcriptional regulator integrating
533 endogenous with environmental signals to determine the outgrowth of tiller buds. Based on
534 the microarray hybridization experiment *INT-C* dependent genes are defined.

535

536 ***INT-C* integrates environmental signals to regulate tiller bud outgrowth**

537 In crop plants, tillering is an important agronomic trait for yield formation. However, in
538 barley little is known about the genetic mechanisms acting inside tiller buds to cause growth
539 arrest. Here, we show that the bHLH transcription factor *INTERMEDIUM-C* (*INT-C*) is
540 involved in the integration of different branching signals mediating a suppressive effect on
541 bud outgrowth (Figure 3). *INT-C* itself is regulated on the transcriptional level as response of
542 the investigated environmental conditions. This modulation of *INT-C* transcription appears to
543 be under tight regulation of environmental and developmental stimuli that are correlated with
544 bud outgrowth and activation of tillering. *INT-C* upregulation was observed after shading or
545 under high planting densities (Figure 3, 4), linked to reduced tiller numbers; on the contrary
546 suppression of *INT-C* expression, i.e., after decapitation, triggered bud outgrowth (Figure 5).
547 This emphasizes a role of *INT-C* as a regulator integrating signals within the axillary bud to
548 determine tiller number. This finding agrees with the results in rice where TB1 was also

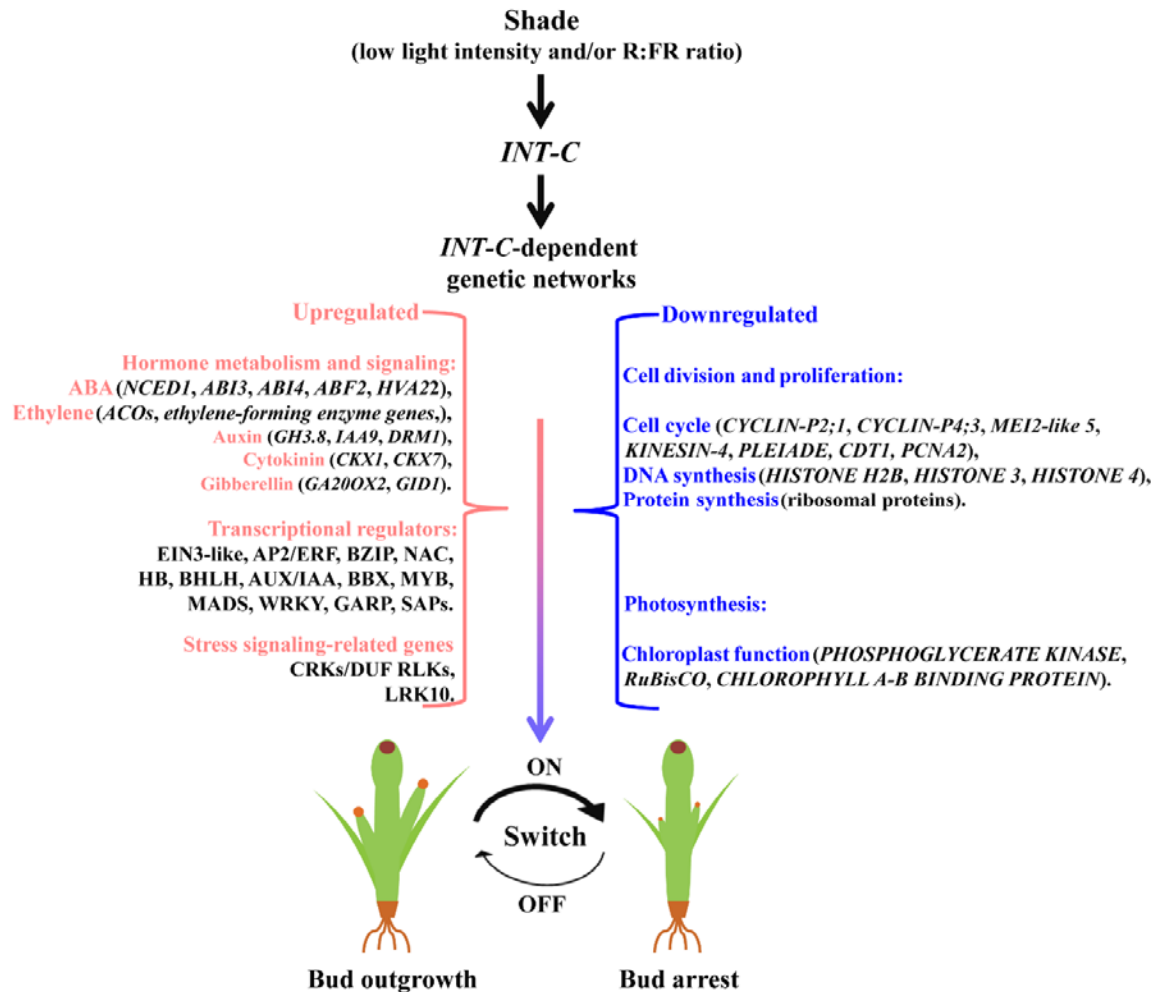
549 reported to mediate a negative function in tillering (Takeda et al., 2003; Choi et al., 2012). A
550 comparable approach using transgenic overexpression and antisense mediated repression of
551 INT-C resulted in the modulation of tiller and panicle development in rice. The influence and
552 integration of environmental stimuli in rice was only addressed in response to greenhouse and
553 paddy field conditions. In maize the involvement of the SPL gene family as direct regulators
554 of TB1 on plant architectural traits was described and optimized plants were engineered for
555 high-density planting (Wei et al., 2018).

556

557 **Definition of *INT-C*-dependent genes**

558

559 The analysis of the shading response at the transcriptome level led to the identification of
560 important differentially expressed genes that were directly or indirectly dependent on INT-C.
561 Our data suggest that the number of INT-C-dependent genes (229 up- and 82 downregulated)
562 was closely associated with tiller bud activation, confirmed through *int-c* mutant study, and
563 INT-C function inferred from the stimulus experiments (either shade or decapitation). These
564 target genes are promising candidates to play an important role in tiller bud transition between
565 repression and promotion of growth. The MAPMAN-based categorization of DEGs resulted
566 in a significant overrepresentation of the term thylakoid and genes associated with
567 photosynthesis. In addition to this, several target genes of sink/source properties of a tissue
568 are found (e.g. TPS6, sucrose transporters). This supports the idea of bud activation,
569 accompanied by generation of a new initial sink tissue. Also, photosynthesis will be activated
570 in this new formed tiller. The scheme in Figure 7 show the integration of the respective
571 categories and important genes involved in INT-C mediated bud activation.



572
573
574
575
576
577
578

Figure 7. Working model for the dynamic balance of INT-C-dependent transcriptional programming to regulate tiller bud outgrowth in barley. Shade perception occurring in tiller bud activates the “master-switch” transcription factor *INT-C*, thus altering INT-C-dependent target genes, among them is a set of upregulated hormone and stress-response genes and down-regulated cell division- and ribosome-related genes. The output of this transcriptional regulation mediates bud transition from outgrowth to arrest.

579 ABA signaling and the promotion of bud dormancy

580 ABA has been related to the maintenance and promotion of bud dormancy in many plant
581 species: elevated ABA levels in buds are associated with the inhibition of branching during
582 plant development (Tamas et al., 1979; Knox and Wareing, 1984; Gocal et al., 1991; Mader et
583 al., 2003; Destefano-Beltran et al., 2006; Ruttink et al., 2007; Eggert and von Wiren, 2017), as
584 well as in the context of responses to low R:FR ratios (Tucker and Mansfield, 1971; Reddy et
585 al., 2013; Gonzalez-Grandio et al., 2017). Moreover, a correlation has been found between the
586 upregulation of ABA-response genes in axillary buds and bud dormancy (Ruttink et al., 2007;
587 Gonzalez-Grandio et al., 2013; Kebrom and Mullet, 2016). So far, neither ABA
588 measurements have been reported in tiller buds, nor ABA-inducible genes have been studied
589 in the tiller bud development of barley (Hussien et al., 2014). Nonetheless, it has been

590 supposed that in barley a correlation exists between ABA signaling and bud arrest
591 (Finkelstein, 2013). Recently, (Luo et al., 2019) and colleagues have shown that application
592 of ABA to hydroponic cultures of rice strigolactone mutants and wild-type plants suppressed
593 axillary bud outgrowth. Strigolactone and ABA biosynthesis share the same precursor and are
594 closely related in regulating the tiller number in barley (Wang et al., 2018). In the present
595 study we demonstrate that INT-C as regulatory hub regulates various ABA hormone pathway
596 genes as well decapitation and shade responses. The large number of transcription factors
597 found in the list of defined INT-C-dependent genes also points toward a function of *INT-C* as
598 regulatory hub controlling a complex downstream network. Our transcript data provide
599 evidence that wild-type tiller buds display a strong increase in the global response of ABA-
600 related genes, while *int-c* buds, which exhibit less dormancy and continue to grow, show
601 reduced ABA-related responses. Consistently, the number of ABA-related genes in the tiller
602 buds was higher after shading. These findings are subsumed in the model (Figure 7) building
603 the hypothesis that INT-C employs the ABA signaling pathway in conjunction with other
604 hormones to mediate bud growth arrest.

605

606 **Author contributions:** H.W. planned and designed the research. H.W. performed
607 experiments and H.W., C.S. and M.K. analyzed the data. H.W., M.K., N. S, and N.v.W.
608 conceived the study. H.W. and M.K wrote the manuscript.

609

610 **Funding information:** This work was supported by IZN (Interdisciplinary Centre for Crop
611 Plant Research), Halle (Saale), Saxony-Anhalt, Germany and the Leibniz Graduate School
612 “Yield Formation in cereals-overcoming yield-limiting factors” IPK. We thank Barbara
613 Kettig, IPK Gatersleben, for excellent technical assistance.

614

615 **References**

- 616 **Aguilar-Martinez JA, Poza-Carrion C, Cubas P** (2007) Arabidopsis BRANCHED1 acts as an integrator of
617 branching signals within axillary buds. *Plant Cell* **19**: 458-472
- 618 **Ballare CL** (1999) Keeping up with the neighbours: phytochrome sensing and other signalling
619 mechanisms (vol 4, pg 97, 1999). *Trends in Plant Science* **4**: 201-201
- 620 **Braun N, de Saint Germain A, Pillot JP, Boutet-Mercey S, Dalmais M, Antoniadis I, Li X, Maia-
621 Grondard A, Le Signor C, Bouteiller N, Luo D, Bendahmane A, Turnbull C, Rameau C** (2012)
622 The Pea TCP Transcription Factor PsBRC1 Acts Downstream of Strigolactones to Control
623 Shoot Branching. *Plant Physiology* **158**: 225-238
- 624 **Casal JJ, Sanchez RA, Deregibus VA** (1986) The Effect of Plant-Density on Tillering - the Involvement
625 of R/Fr Ratio and the Proportion of Radiation Intercepted Per Plant. *Environmental and
626 Experimental Botany* **26**: 365-371
- 627 **Chen M, Chory J, Fankhauser C** (2004) Light signal transduction in higher plants. *Annual Review of
628 Genetics* **38**: 87-117

- 629 **Choi MS, Woo MO, Koh EB, Lee J, Ham TH, Seo HS, Koh HJ** (2012) Teosinte Branched 1 modulates
630 tillering in rice plants. *Plant Cell Rep* **31**: 57-65
- 631 **Cline MG** (1997) Concepts and terminology of apical dominance. *American Journal of Botany* **84**:
632 1064-1069
- 633 **Cline MG** (2000) Execution of the auxin replacement apical dominance experiment in temperate
634 woody species. *American Journal of Botany* **87**: 182-190
- 635 **Destefano-Beltran L, Knauber D, Huckle L, Suttle J** (2006) Chemically forced dormancy termination
636 mimics natural dormancy progression in potato tuber meristems by reducing ABA content
637 and modifying expression of genes involved in regulating ABA synthesis and metabolism.
638 *Journal of Experimental Botany* **57**: 2879-2886
- 639 **Devlin PF, Yanovsky MJ, Kay SA** (2003) A genomic analysis of the shade avoidance response in
640 *Arabidopsis*. *Plant Physiology* **133**: 1617-1629
- 641 **Doebley J, Stec A, Hubbard L** (1997) The evolution of apical dominance in maize. *Nature* **386**: 485-
642 488
- 643 **Duek PD, Fankhauser C** (2005) bHLH class transcription factors take centre stage in phytochrome
644 signalling. *Trends in Plant Science* **10**: 51-54
- 645 **Eggert K, von Wiren N** (2017) Response of the plant hormone network to boron deficiency. *New*
646 *Phytol* **216**: 868-881
- 647 **Franklin KA, Quail PH** (2010) Phytochrome functions in *Arabidopsis* development. *Journal of*
648 *Experimental Botany* **61**: 11-24
- 649 **Gocal GFW, Pharis RP, Yeung EC, Pearce D** (1991) Changes after Decapitation in Concentrations of
650 Indole-3-Acetic-Acid and Abscisic-Acid in the Larger Axillary Bud of *Phaseolus-Vulgaris* L-Cv
651 Tender Green. *Plant Physiology* **95**: 344-350
- 652 **Gonzalez-Grandio E, Pajoro A, Franco-Zorrilla JM, Tarancon C, Immink RGH, Cubas P** (2017) Abscisic
653 acid signaling is controlled by a BRANCHED1/HD-ZIP I cascade in *Arabidopsis* axillary buds.
654 *Proceedings of the National Academy of Sciences of the United States of America* **114**: E245-
655 E254
- 656 **Gonzalez-Grandio E, Poza-Carrion C, Sorzano CO, Cubas P** (2013) BRANCHED1 promotes axillary bud
657 dormancy in response to shade in *Arabidopsis*. *Plant Cell* **25**: 834-850
- 658 **Hall SM, Hillman JR** (1975) Correlative Inhibition of Lateral Bud Growth in *Phaseolus-Vulgaris* L
659 Timing of Bud Growth Following Decapitation. *Planta* **123**: 137-143
- 660 **Hornitschek P, Kohnen MV, Lorrain S, Rougemont J, Ljung K, Lopez-Vidriero I, Franco-Zorrilla JM,**
661 **Solano R, Trevisan M, Pradervand S, Xenarios I, Fankhauser C** (2012) Phytochrome
662 interacting factors 4 and 5 control seedling growth in changing light conditions by directly
663 controlling auxin signaling. *Plant Journal* **71**: 699-711
- 664 **Howarth DG, Donoghue MJ** (2006) Phylogenetic analysis of the "ECE" (CYC/TB1) clade reveals
665 duplications predating the core eudicots. *Proceedings of the National Academy of Sciences of*
666 *the United States of America* **103**: 9101-9106
- 667 **Hussien A, Tavakol E, Horner DS, Munoz-Amatriain M, Muehlbauer GJ, Rossini L** (2014) Genetics of
668 Tillering in Rice and Barley. *Plant Genome* **7**
- 669 **Kang YH, Khan S, Ma XY** (2009) Climate change impacts on crop yield, crop water productivity and
670 food security - A review. *Progress in Natural Science-Materials International* **19**: 1665-1674
- 671 **Kebrom TH, Brutnell TP, Finlayson SA** (2010) Suppression of sorghum axillary bud outgrowth by
672 shade, phyB and defoliation signalling pathways. *Plant Cell and Environment* **33**: 48-58
- 673 **Kebrom TH, Burson BL, Finlayson SA** (2006) Phytochrome B represses Teosinte Branched1
674 expression and induces sorghum axillary bud outgrowth in response to light signals. *Plant*
675 *Physiology* **140**: 1109-1117
- 676 **Kebrom TH, Mullet JE** (2016) Transcriptome Profiling of Tiller Buds Provides New Insights into PhyB
677 Regulation of Tillering and Indeterminate Growth in Sorghum. *Plant Physiology* **170**: 2232-
678 2250
- 679 **Kebrom TH, Spielmeier W, Finnegan EJ** (2013) Grasses provide new insights into regulation of shoot
680 branching. *Trends in Plant Science* **18**: 41-48

- 681 **Kegge W, Weldegergis BT, Soler R, Vergeer-Van Eijk M, Dicke M, Voesenek LACJ, Pierik R** (2013)
682 Canopy light cues affect emission of constitutive and methyl jasmonate-induced volatile
683 organic compounds in *Arabidopsis thaliana*. *New Phytologist* **200**: 861-874
- 684 **Knox JP, Wareing PF** (1984) Apical Dominance in *Phaseolus-Vulgaris* L - the Possible Roles of Abscisic
685 and Indole-3-Acetic-Acid. *Journal of Experimental Botany* **35**: 239-244
- 686 **Kong LS, Abrams SR, Owen SJ, Graham H, von Aderkasi P** (2008) Phytohormones and their
687 metabolites during long shoot development in Douglas-fir following cone induction by
688 gibberellin injection. *Tree Physiology* **28**: 1357-1364
- 689 **Koppolu R, Anwar N, Sakuma S, Tagiri A, Lundqvist U, Pourkheirandish M, Rutten T, Seiler C,**
690 **Himmelbach A, Ariyadasa R, Youssef HM, Stein N, Sreenivasulu N, Komatsuda T,**
691 **Schnurbusch T** (2013) Six-rowed spike4 (*Vrs4*) controls spikelet determinacy and row-type in
692 barley. *Proc Natl Acad Sci U S A* **110**: 13198-13203
- 693 **Kosugi S, Ohashi Y** (1997) PCF1 and PCF2 specifically bind to cis elements in the rice proliferating cell
694 nuclear antigen gene. *Plant Cell* **9**: 1607-1619
- 695 **Leivar P, Monte E** (2014) PIFs: Systems Integrators in Plant Development. *Plant Cell* **26**: 56-78
- 696 **Li S** (2015) The *Arabidopsis thaliana* TCP transcription factors: A broadening horizon beyond
697 development. *Plant Signal Behav* **10**: e1044192
- 698 **Liller CB, Neuhaus R, von Korff M, Koornneef M, van Esse W** (2015) Mutations in Barley Row Type
699 Genes Have Pleiotropic Effects on Shoot Branching. *Plos One* **10**
- 700 **Livak KJ, Schmittgen TD** (2001) Analysis of relative gene expression data using real-time quantitative
701 PCR and the 2(T)(-Delta Delta C) method. *Methods* **25**: 402-408
- 702 **Luo D, Carpenter R, Vincent C, Copsey L, Coen E** (1996) Origin of floral asymmetry in *Antirrhinum*.
703 *Nature* **383**: 794-799
- 704 **Luo L, Takahashi M, Kameoka H, Qin R, Shiga T, Kanno Y, Seo M, Ito M, Xu G, Kyojuka J** (2019)
705 Developmental analysis of the early steps in strigolactone-mediated axillary bud dormancy in
706 rice. *Plant J* **97**: 1006-1021
- 707 **Mader JC, Emery RJN, Turnbull CGN** (2003) Spatial and temporal changes in multiple hormone
708 groups during lateral bud release shortly following apex decapitation of chickpea (*Cicer*
709 *arietinum*) seedlings. *Physiologia Plantarum* **119**: 295-308
- 710 **Martin-Trillo M, Cubas P** (2010) TCP genes: a family snapshot ten years later. *Trends Plant Sci* **15**: 31-
711 39
- 712 **Martin-Trillo M, Grandio EG, Serra F, Marcel F, Rodriguez-Buey ML, Schmitz G, Theres K,**
713 **Bendahmane A, Dopazo H, Cubas P** (2011) Role of tomato BRANCHED1-like genes in the
714 control of shoot branching. *Plant Journal* **67**: 701-714
- 715 **Minakuchi K, Kameoka H, Yasuno N, Umehara M, Luo L, Kobayashi K, Hanada A, Ueno K, Asami T,**
716 **Yamaguchi S, Kyojuka J** (2010) FINE CULM1 (FC1) Works Downstream of Strigolactones to
717 Inhibit the Outgrowth of Axillary Buds in Rice. *Plant and Cell Physiology* **51**: 1127-1135
- 718 **Napoli CA, Beveridge CA, Snowden KC** (1999) Reevaluating concepts of apical dominance and the
719 control of axillary bud outgrowth. *Current Topics in Developmental Biology*, Vol 44 **44**: 127-
720 169
- 721 **Nath U, Crawford BCW, Carpenter R, Coen E** (2003) Genetic control of surface curvature. *Science*
722 **299**: 1404-1407
- 723 **Ori N, Cohen AR, Etzioni A, Brand A, Yanai O, Shleizer S, Menda N, Amsellem Z, Efroni I, Pekker I,**
724 **Alvarez JP, Blum E, Zamir D, Eshed Y** (2007) Regulation of LANCEOLATE by miR319 is
725 required for compound-leaf development in tomato. *Nature Genetics* **39**: 787-791
- 726 **Ozhuner E, Eldem V, Ipek A, Okay S, Sakcali S, Zhang B, Boke H, Unver T** (2013) Boron stress
727 responsive microRNAs and their targets in barley. *PLoS One* **8**: e59543
- 728 **Palatnik JF, Allen E, Wu XL, Schommer C, Schwab R, Carrington JC, Weigel D** (2003) Control of leaf
729 morphogenesis by microRNAs. *Nature* **425**: 257-263
- 730 **Palatnik JF, Wollmann H, Schommer C, Schwab R, Boisbouvier J, Rodriguez R, Warthmann N, Allen**
731 **E, Dezulian T, Huson D, Carrington JC, Weigel D** (2007) Sequence and expression differences
732 underlie functional specialization of *Arabidopsis* MicroRNAs miR159 and miR319.
733 *Developmental Cell* **13**: 115-125

- 734 **Quevillon E, Silventoinen V, Pillai S, Harte N, Mulder N, Apweiler R, Lopez R** (2005) InterProScan:
735 protein domains identifier. *Nucleic Acids Research* **33**: W116-W120
- 736 **Ramsay L, Comadran J, Druka A, Marshall DF, Thomas WT, Macaulay M, MacKenzie K, Simpson C,**
737 **Fuller J, Bonar N, Hayes PM, Lundqvist U, Franckowiak JD, Close TJ, Muehlbauer GJ, Waugh**
738 **R** (2011) INTERMEDIUM-C, a modifier of lateral spikelet fertility in barley, is an ortholog of
739 the maize domestication gene TEOSINTE BRANCHED 1. *Nat Genet* **43**: 169-172
- 740 **Reddy SK, Holalu SV, Casal JJ, Finlayson SA** (2013) Abscisic Acid Regulates Axillary Bud Outgrowth
741 Responses to the Ratio of Red to Far-Red Light. *Plant Physiology* **163**: 1047-1058
- 742 **Reed JW, Nagpal P, Poole DS, Furuya M, Chory J** (1993) Mutations in the Gene for the Red Far-Red
743 Light Receptor Phytochrome-B Alter Cell Elongation and Physiological-Responses Throughout
744 Arabidopsis Development. *Plant Cell* **5**: 147-157
- 745 **Ruttink T, Arend M, Morreel K, Storme V, Rombauts S, Fromm J, Bhalerao RP, Boerjan W, Rohde A**
746 (2007) A molecular timetable for apical bud formation and dormancy induction in poplar.
747 *Plant Cell* **19**: 2370-2390
- 748 **Skinner RH, Simmons SR** (1993) Modulation of Leaf Elongation, Tiller Appearance and Tiller
749 Senescence in Spring Barley by Far-Red Light. *Plant Cell and Environment* **16**: 555-562
- 750 **Smith H** (2000) Phytochromes and light signal perception by plants--an emerging synthesis. *Nature*
751 **407**: 585-591
- 752 **Smith JE, Jordan PW** (1994) Stand Density Effects on Branching in an Annual Legume (*Senna-*
753 *Obtusifolia*). *Annals of Botany* **74**: 17-25
- 754 **Stafstrom JP, Ripley BD, Devitt ML, Drake B** (1998) Dormancy-associated gene expression in pea
755 axillary buds. *Planta* **205**: 547-552
- 756 **Stamm P, Kumar PP** (2010) The phytohormone signal network regulating elongation growth during
757 shade avoidance. *J Exp Bot* **61**: 2889-2903
- 758 **Takeda T, Suwa Y, Suzuki M, Kitano H, Ueguchi-Tanaka M, Ashikari M, Matsuoka M, Ueguchi C**
759 (2003) The OsTB1 gene negatively regulates lateral branching in rice. *Plant J* **33**: 513-520
- 760 **Tamas IA, Ozbun JL, Wallace DH, Powell LE, Engels CJ** (1979) Effect of Fruits on Dormancy and
761 Abscisic-Acid Concentration in the Axillary Buds of *Phaseolus-Vulgaris* L. *Plant Physiology* **64**:
762 615-619
- 763 **Tamura K, Stecher G, Peterson D, Filipski A, Kumar S** (2013) MEGA6: Molecular Evolutionary
764 Genetics Analysis Version 6.0. *Molecular Biology and Evolution* **30**: 2725-2729
- 765 **Tao Y, Ferrer JL, Ljung K, Pojer F, Hong FX, Long JA, Li L, Moreno JE, Bowman ME, Ivans LJ, Cheng YF,**
766 **Lim J, Zhao YD, Ballare CL, Sandberg G, Noel JP, Chory J** (2008) Rapid synthesis of auxin via a
767 new tryptophan-dependent pathway is required for shade avoidance in plants. *Cell* **133**: 164-
768 176
- 769 **Tatematsu K, Ward S, Leyser O, Kamiya Y, Nambara E** (2005) Identification of cis-elements that
770 regulate gene expression during initiation of axillary bud outgrowth in arabidopsis. *Plant*
771 *Physiology* **138**: 757-766
- 772 **Thimm O, Blasing O, Gibon Y, Nagel A, Meyer S, Kruger P, Selbig J, Muller LA, Rhee SY, Stitt M**
773 (2004) MAPMAN: a user-driven tool to display genomics data sets onto diagrams of
774 metabolic pathways and other biological processes. *Plant J* **37**: 914-939
- 775 **Thirulogachandar V, Alqudah AM, Koppolu R, Rutten T, Graner A, Hensel G, Kumlehn J, Brautigam**
776 **A, Sreenivasulu N, Schnurbusch T, Kuhlmann M** (2017) Leaf primordium size specifies leaf
777 width and vein number among row-type classes in barley. *Plant J* **91**: 601-612
- 778 **Thompson JD, Gibson TJ, Plewniak F, Jeanmougin F, Higgins DG** (1997) The CLUSTAL_X windows
779 interface: flexible strategies for multiple sequence alignment aided by quality analysis tools.
780 *Nucleic Acids Research* **25**: 4876-4882
- 781 **Thompson JD, Higgins DG, Gibson TJ** (1994) Clustal-W - Improving the Sensitivity of Progressive
782 Multiple Sequence Alignment through Sequence Weighting, Position-Specific Gap Penalties
783 and Weight Matrix Choice. *Nucleic Acids Research* **22**: 4673-4680
- 784 **Tian T, Liu Y, Yan HY, You Q, Yi X, Du Z, Xu WY, Su Z** (2017) agriGO v2.0: a GO analysis toolkit for the
785 agricultural community, 2017 update. *Nucleic Acids Research* **45**: W122-W129

- 786 **Tucic B, Ducic J, Pemac D** (2006) Phenotypic responses to early signals of neighbour proximity in
787 *Picea omorika*, a pioneer conifer tree. *Basic and Applied Ecology* **7**: 443-454
- 788 **Tucker DJ, Mansfield TA** (1971) Effects of light quality on apical dominance in *Xanthium strumarium*
789 and the associated changes in endogenous levels of abscisic acid and cytokinins. *Planta* **102**:
790 140-151
- 791 **Usadel B, Nagel A, Thimm O, Redestig H, Blaesing OE, Palacios-Rojas N, Selbig J, Hannemann J,**
792 **Piques MC, Steinhäuser D, Scheible WR, Gibon Y, Morcuende R, Weicht D, Meyer S, Stitt M**
793 (2005) Extension of the visualization tool MapMan to allow statistical analysis of arrays,
794 display of corresponding genes, and comparison with known responses. *Plant Physiol* **138**:
795 1195-1204
- 796 **Wang H, Wang HY** (2015) Phytochrome Signaling: Time to Tighten up the Loose Ends. *Molecular*
797 *Plant* **8**: 540-551
- 798 **Wang H, Wu GX, Zhao BB, Wang BB, Lang ZH, Zhang CY, Wang HY** (2016) Regulatory modules
799 controlling early shade avoidance response in maize seedlings. *Bmc Genomics* **17**
- 800 **Wang HW, Chen WX, Eggert K, Charnikhova T, Bouwmeester H, Schweizer P, Hajirezaei MR, Seiler**
801 **C, Sreenivasulu N, von Wiren N, Kuhlmann M** (2018) Abscisic acid influences tillering by
802 modulation of strigolactones in barley. *Journal of Experimental Botany* **69**: 3883-3898
- 803 **Wei H, Zhao Y, Xie Y, Wang H** (2018) Exploiting SPL genes to improve maize plant architecture
804 tailored for high-density planting. *J Exp Bot* **69**: 4675-4688
- 805 **Whipple CJ, Kebrom TH, Weber AL, Yang F, Hall D, Meeley R, Schmidt R, Doebley J, Brutnell TP,**
806 **Jackson DP** (2011) grassy tillers1 promotes apical dominance in maize and responds to shade
807 signals in the grasses. *Proceedings of the National Academy of Sciences of the United States*
808 *of America* **108**: E506-E512
- 809 **Yao X, Ma H, Wang J, Zhang DB** (2007) Genome-wide comparative analysis and expression pattern of
810 TCP gene families in *Arabidopsis thaliana* and *Oryza sativa*. *Journal of Integrative Plant*
811 *Biology* **49**: 885-897
- 812 **Zadoks JC** (1985) Citation Classic - a Decimal Code for the Growth-Stages of Cereals. *Current*
813 *Contents/Agriculture Biology & Environmental Sciences*: 14-14
- 814 **Zimmermann P, Hirsch-Hoffmann M, Hennig L, Gruissem W** (2004) GENEVESTIGATOR. *Arabidopsis*
815 *microarray database and analysis toolbox*. *Plant Physiology* **136**: 2621-2632

816
817
818
819

820 **Supplemental Information**

821 **Supplemental Figure S1.** Flowering in wild type and *int-c* mutant plants at 15 weeks after
822 germination. Shown
823 are three independent replicates for each.

824
825 **Supplemental Figure S2.** Validation of microarray data by qRT-PCR after decapitation treatment. A
826 mRNA levels of a subset of genes identified as responding to the decapitation treatment both in wild-
827 type and *int-c* samples. C and D, Pearson's correlations between gene expression levels determined by
828 qRT-PCR and microarray expression profiling for the same genes. Although the correlations of both
829 datasets are high, microarray data underestimate the degree of change. The qRT-PCR and microarray
830 data showed a very high average Pearson correlation coefficient (0,9107; confirming the high
831 reliability of the array data.

832 **Supplemental Figure S3.** Validation of microarray data by qRT-PCR. A and B, mRNA levels of a
833 subset of genes identified as responding to the shade treatment both in wild-type and *int-c* samples. C
834 and D, Pearson's correlations between gene expression levels determined by qRT-PCR and microarray
835 expression profiling for the same genes. Although the correlations of both datasets are high,
836 microarray data underestimate the degree of change. The qRT-PCR and microarray data showed a

837 very high average Pearson correlation coefficient (0.85 and 0.81 for the wild type and *int-c*,
838 respectively; confirming the high reliability of the array data.

839

840 **Supplemental Figure S4. Selected** MAPMAN-based categorization of DEGs

841

842

843 **Supplementary table 1:** List of TCP genes and associated gene expression derived from public
844 databases.

845 **Supplementary table 2:** List of differential expressed genes (DEGs) for WT vs int-c (Control
846 condition), WT vs int-c (shading condition), WT vs WT shading condition, int-c vs int-c shading
847 condition, WT vs WT decapitation condition. Each with a list of associated direction of change.

848 **Supplementary table 3:** List of INT-C dependent genes, including comparison of direction after
849 shading and decapitation.